Application of fourier method to study propagation of compression shock wave in pipelines with damper

O. Sh. Bozorov[1*], *I.* Khujaev[2], *Kh.* Aminov[3], and *Sh.* Khojikulov[2]

[1]Karshi Engineering Economics Institute, Karshi, Uzbekistan
[2]Institute of Mechanics and Seismic Stability of Structures, Tashkent, Uzbekistan
[3]University Oriental, Tashkent state university of oriental studies, Tashkent, Uzbekistan

Abstract. The transition problems from one mode of steady flow to another in a pipeline with a constant gradient are considered. The pressure value is set at the inlet to the section, and an air chamber of a certain volume is installed at the outlet. Modeling of the process of compression shock wave propagation in an elementary section of the pipeline was conducted according to the linearized quasi-one-dimensional N.E. Zhukovskymodel, and the damper was considered according to the I.A. Charny model. The problem is solved by the method of separation of variables. It is shown that at an increase in the volume of the damper, the amplitude and frequency of perturbations decrease due to the transient process.

1 Introduction

Shock wave often occurs in nature and technology and can have a positive or negative effect [1-6]. Its positive effect is used in the work of an air hammer. Multiple repetitions of the shock wave impact can lead to the gradual destruction of equipment since it initiates vibrations of different amplitude and frequencies of excitations. With the rapid closing of the free section of horizontal or inclined pipelines, large pressure surges can form due to the transition of the kinetic energy of the conveyed medium to the potential energy of compression [7-11].

N.E. Zhukovsky obtained the first theoretical and experimental results on the nature of a shock wave in pipelines. His research considered the low compressibility of the conveyed fluid and the deformation of the thin wall of the pipeline under the influence of a shock wave [12]. A quasi-one-dimensional mathematical model of pipeline transportation of fluids and gases under conditions of compaction shockwave propagation is widely used in solving scientific and practical problems.

Various analytical and numerical methods were developed for solving complete or reduced options of linear and nonlinear quasi-one-dimensional equations of pipelines transporting compressible or low-compressible media [12-19]. The analysis showed that few publications are devoted to studying changes in the fluid momentum in inclined

*Corresponding author: shakhboz2016@mail.ru

pipelines. In this article, the slope of the pipeline is assumed to be constant. In addition, the momentum conservation equation considers the local component of the fluid inertia force and the drag force according to the Darcy-Weisbach formula. The continuity equation represents the propagation velocity of small pressure disturbances in the "pipe-fluid" medium.

A pressure value is set at the section inlet, and an air chamber is installed at the outlet. A method for considering the damper in the boundary condition, according to I.A. Charny [12], is shown.

The linearized equation of momentum conservation and transfer is solved by the Fourier method. By substituting the found velocity value into the initial equations, the equations for hydrostatic pressure are derived and integrated.

Numerical results are presented for individual options of the compaction shock wave propagation process.

The purpose of the problem is to study the dynamic state of an elementary section of the pipeline during the transition from one velocity mode to another. A pipeline of length l and diameter D_0. is considered. The slope of the pipeline route $\sin\alpha$ is constant. The initial condition for the velocity is:

$$w(x,0) = w_0 = const\ .$$

The initial pressure distribution takes into account the inlet pressure p_{00}, the difference in pressure due to friction and gravity:

$$p(x,0) = p_{00} - \rho(2aw_0 + g\sin\alpha)x\ .$$

Here $2a = \frac{\lambda w_*}{2D} = const$; $\sin\alpha = \frac{dy}{dx}$; λ –is the drag coefficient; w_* is the characteristic velocity of the object under consideration (in this case, the averaging parameter); $y(x)$ is the leveling height of the pipeline axis.

The following value of pressure is set at the inlet:

$$p(0,t) = p_{00} = const\ .$$

The intensity of fluid withdrawal from the end of the section at $t > 0$ is $Q(t)$ $\left(m^3/s\right)$. An air chamber is installed in front of the exit from the section. In the unperturbed state, the gas volume and pressure in the air chamber are V_0 and p_0. This boundary condition, which reflects the installation of the air chamber, is formulated according to I.A. Charny [12].

In front of the air chamber, the volumetric flow rate of the liquid is $(fw)_{x=l}$, where $f = \pi D^2/4$ is the cross-sectional area and D is the diameter of the pipeline. At the exit, as already noted, the flow rate is $Q(t)$. The difference leads to a change in the volume of gas in the air chamber over time:

$$\frac{dy}{dx} = (fw)_{x=l} - Q(t)\ .$$

When changing the volume of the liquid, the change in the gas temperature can be ignored. Therefore, the new state of air p and $V_0 - y$ satisfy the following condition:

$$p_0 V_0 = p\left(V_0 - y\right).$$

The new pressure value in the air chamber is

$$p = \frac{p_0 V_0}{V_0 - y}.$$

Since the change in y is small $\left(y << V_0\right)$, we can assume that

$$p = \frac{p_0}{1 - y / V_0} \approx p_0\left(1 + \frac{y}{V_0}\right).$$

From here we find $y = \frac{p - p_0}{p_0} V_0$ and

$$\frac{dy}{dt} = \frac{V_0}{p_0}\frac{dp}{dt}.$$

Equating the right sides of two equalities for $\frac{dy}{dt}$, we obtain the following condition at the exit from the section:

$$\frac{V_0}{p_0}\frac{dp_{x=l}}{dt} = \left(fw\right)_{x=l} - Q\left(t\right).$$

We model the equations of state of the section based on the N.E. Zhukovskyequations with correction, considering the force of gravity [12]:

$$\begin{cases} -\frac{\partial p}{\partial x} = \rho\left(\frac{\partial w}{\partial t} + 2aw + g\sin\alpha\right), \\ -\frac{\partial p}{\partial t} = \rho c\ \frac{\partial w}{\partial x}. \end{cases}$$

Here $c^2 = \left(\frac{\rho_0}{k} + \frac{D\rho_0}{E\delta}\right)^{-1/2}$ is the propagation velocity of small perturbations in the "fluid-pipe" system; ρ, k are the density of the fluid at rest and its modulus of elasticity; E, δ are the Young modulus of the pipeline material and the thickness of the pipe $\left(\delta << D\right)$.

Since $\frac{\partial p}{\partial t}$ can be expressed according to the second equation of the system, the second boundary condition of velocity w takes the following form:

$$-\beta \frac{\partial w(l,t)}{\partial t} = w(l,t) - w.$$

When the damper is disabled, this condition becomes a condition of the first kind $w(l,t) = w_A$. Here and below, notation $\beta = \frac{\rho c V}{fp}$ is used.

In general, such a problem statement differs from other problems in that both the slope of the route and the presence of a damper at the end of the section are simultaneously considered.

2 Methods

Let us single out the solution to the problem concerning velocity. The following conditions are valid:

$$w(x,0) = w, \qquad \frac{\partial w(x,0)}{\partial t} = 0,$$

$$\frac{\partial w(0,t)}{\partial x} = 0, \qquad \beta \frac{\partial w(l,t)}{\partial x} + w(l,t) = w_A$$

where we confine ourselves to considering the case when the new rate at the exit from the section is w_A.

From the original system, the telegraph equation is derived [13-14]:

$$\frac{\partial^2 w}{\partial t^2} + 2a \frac{\partial w}{\partial t} = c^2 \frac{\partial^2 w}{\partial x^2}.$$

To apply the Fourier method, the boundary conditions of the problem must be reduced to a homogeneous form. In our case, this is possible if we accept the following replacement

$$u(x,t) = w(x,t) - w_A.$$

In this case, the equations, initial conditions, and the first boundary condition are written in terms of $u(x,t)$, and the second boundary condition acquires a homogeneous form:

$$\frac{\partial u(l,t)}{\partial x} + \frac{1}{\beta} u(l,t) = 0.$$

The solution to $u(x,t)$ is sought in the following form:

$$u(x,t) = X(x)Y(t).$$

Then, according to the rules of the Fourier method [13-14], we obtain

$$\frac{Y''(t)+2aY'(t)}{Y(t)}=\frac{X''(x)}{X(x)}=-\lambda^2 .$$

Here $\lambda>0$, otherwise, we obtain a trivial (zero) solution to the problem.

Let us make an autonomous equation for $X(x)$:

$$X''(x)+\lambda^2 X'(x)=0 .$$

Its solution is sought in the form

$$X(x)=B\sin\lambda x+C\cos\lambda x .$$

The implementation of the boundary conditions leads to partial eigenfunctions:

$$X_n(x)=\cos\lambda_n x$$

where the eigenvalues λ_n of the problem are the positive roots of the characteristic equation

$$tg\lambda_n l=\frac{1}{\beta\lambda} .$$

Theorthonormalityofeigenfunctions $X_n(x)$ was proved:

$$\int_0^l \sin\lambda_n x\sin\lambda_m x dx=\begin{cases}\left\|X_n(x)\right\|^2=\frac{1}{2}\left(l+\beta\sin^2\lambda_n l\right) & for\ n=m,\\ 0 & for\ n\neq m.\end{cases}$$

The search for eigenfunctions in time led to the following equation:

$$Y_n''(t)+2aY_n'(t)+c^2\lambda_n{}^2Y_n(t)=0 .$$

The characteristic equation of the second-order differential equation is:

$$s_n{}^2+2as_n+c^2\lambda_n{}^2=0 .$$

With $D_n=a^2-c^2\lambda_n{}^2$, we obtain

$$(s_n)_{1,2}=-a\pm\sqrt{D_n} .$$

Here we have:

$$Y_n(t)=\begin{cases} e^{-at}\left(A_n ch\sqrt{D_n}t+B_n sh\sqrt{D_n}t\right) & for\ D_n>0,\\ e^{-at}\left(A_n+B_n t\right) & for\ D_n=0,\\ e^{-at}\left(A_n\cos\sqrt{|D_n|}t+B_n\sin\sqrt{|D_n|}t\right) & for\ D_n<0. \end{cases}$$

Thus, the solution $u(x,t)$ is

$$u(x,t)=\sum_{n=1}^{\infty}\frac{\sin\lambda_n l}{\lambda_n\|X_n\|^2}\begin{bmatrix} e^{-at}\left(A_n ch\sqrt{D_n}t+B_n sh\sqrt{D_n}t\right) & for\ D_n>0\\ e^{-at}\left(A_n+B_n t\right) & for\ D_n=0\\ e^{-at}\left(A_n\cos\sqrt{|D_n|}t+B_n\sin\sqrt{|D_n|}t\right) & for\ D_n<0 \end{bmatrix}\cos\lambda_n x.$$

In a partial case as $\beta\to 0$ (i.e. as $V_0\to 0$) under condition $X_n'(0)=0$, the eigenfunctionsare $X_n(x)=\cos\lambda_n x$ for $\lambda_n=\frac{2n-1}{2}\frac{\pi}{l}$ [7]. At the same time, it is assumed that $\|X_n(l)\|^2=\frac{l}{2}$

For $\beta\neq 0$, the eigenvalues of λ_n are found by numerically solving the characteristic equation. First, we singled out the boundary of the membership interval of the n-th root $(n-1)\pi<\lambda_n\le(n-0{,}5)\pi$. Then, the values of $\lambda_n l$ were refined by the dichotomy method [20]. Here, the largest number of approximation steps 42 was sufficient to ensure the calculation accuracy λ_n up to 10^{-10} for $l=1000$ m.

To determine the hydrostatic pressure, the second equation of the original system was integrated over time from 0 to t:

$$p(x,t)=p(x,0)-\rho c^2\int_0^t\frac{\partial w(x,\theta)}{\partial x}d\theta\,.$$

The minuend is known from the initial condition. The subtrahend is calculated from the newly obtained expression for $w(x,t)$. Omitting details, the result has the following form

$$p(x,t)=p_{00}-\rho(2aw_{00}+g\sin\alpha)x-\rho(w_0-w_A)\sum_{n=1}^{\infty}\frac{\sin\lambda_n l}{\lambda_n\|X_n(x)\|^2}\times$$
$$\times\begin{bmatrix} e^{-at}\left(A_n ch\sqrt{D_n}t+B_n sh\sqrt{D_n}t\right) & for\ D_n>0\\ e^{-at}\left(A_n+B_n t\right) & for\ D_n=0\\ e^{-at}\left(A_n\cos\sqrt{|D_n|}t+B_n\sin\sqrt{|D_n|}t\right) & for\ D_n<0 \end{bmatrix}\sin\lambda_n x.$$

3 Results and Discussion

Based on the presented material, a calculation program was compiled in the Pascal ABC environment and the results were presented in tables. Graphs were plotted using the Excel-2003 program. The characteristic equation was solved by the dichotomy method with an

accuracy of 10^{-9}. The calculations considered the first 500 first terms of the Fourier series. The step along the length of the section was $l/50$, and the time step was $l/(10c)$. The calculation was conducted from the 0th to the 600th time step.

Cases $\sin\alpha = 0,\ \pm 0.1$ were considered at a section length of 1000 m. The section diameter was 20 cm, and the drag coefficient $\lambda = 0.018$. The averaging parameter had the value of $w_* = 5\ m/s$, the density of the fluid in the undisturbed state was 1000.0 kg/m^3, and the propagation velocity of small perturbations of pressure was $c = 1200\ m/s$.

The volume of the air chamber connected to the end of the section was taken as 1.0, 0.1, 0.001, 0.0001, and 0.00001 cubic meters. The pressure in the air chamber without stress was $p_0 = 0{,}1\ MPa$.

Let us dwell on the results obtained for a horizontal pipeline for $V_0 = 0.001\ m^3$.

Figure 1 shows the velocity graphs from the 0th to the 10th time step, during which the perturbation wave runs from the end of the section to its beginning (the conditional half-cycle is $\tau = l/c$).

At the initial time, the velocity is zero. When the outlet end is opened, the velocity at the end of the section gradually increases, and the disturbance moves toward the inlet chamber. This is due to the presence of an air chamber. In the absence of an air chamber, an instantaneous increase in velocity up to w_A is expected, and the leading edge makes a surge.

At $t = \tau$, the wave reaches the entrance section (the upper curve in Fig. 1 and the lower curve in Fig. 2).

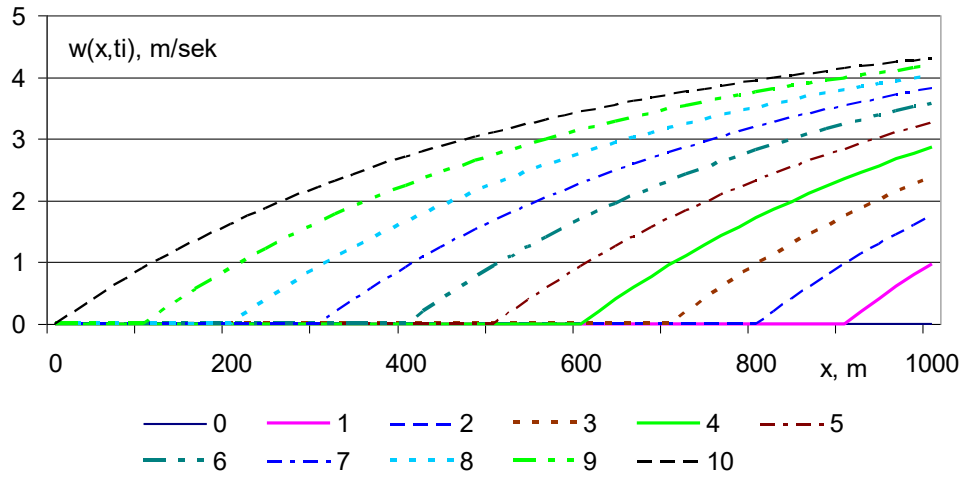

Fig. 1. Velocity profiles at 0-10th time points with $l/(10c)$ step. See data in text.

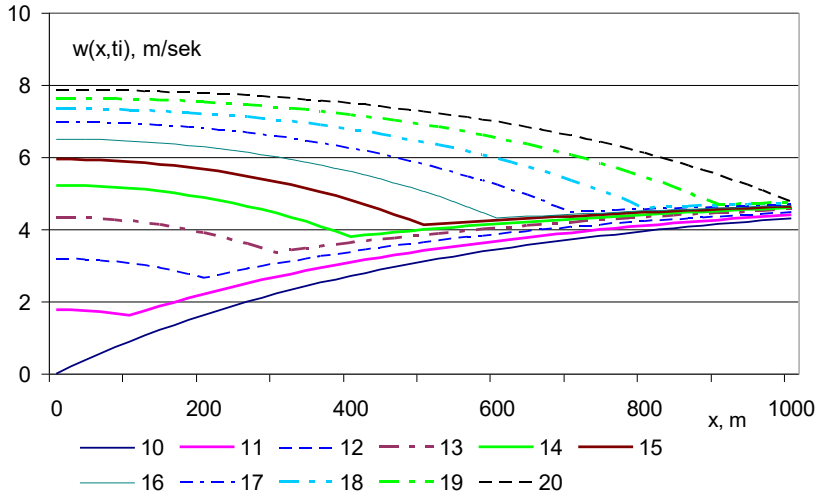

Fig. 2. Velocity profiles at 10-20th time points with $l/(10c)$ step. See data in text.

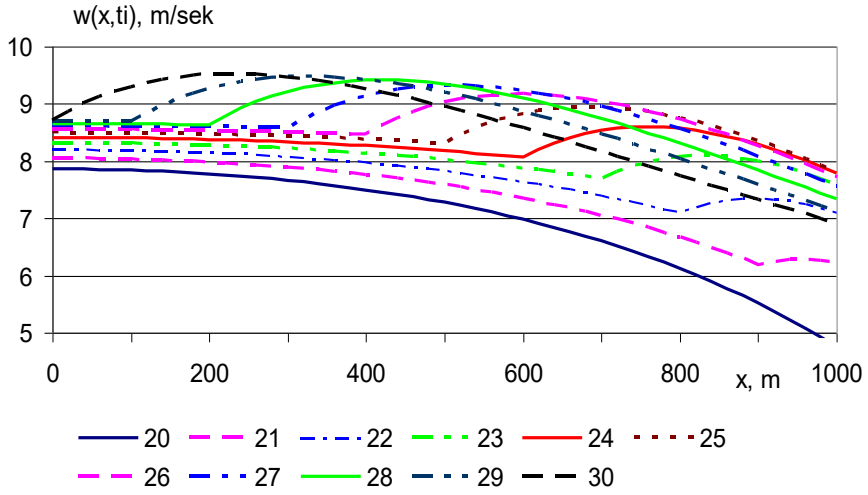

Fig. 3. Velocity profiles for $2l/c \le t \le 3l/c$ with $l/(10c)$ step.

In the inlet section, the condition of pressure constancy $p(0,t) = p_{00} = const.$ is imposed. In connection with this, the velocity disturbances reaching the inlet section lead to an increase in the departure of the disturbance velocity back toward the end of the section. The curve $w(x,\tau)$ practically constitutes a conditional envelope of the velocity curves in the considered time interval $(l/c;\ 2l/c)$. The conditionality lies in the fact that the parts of the curve $w(x,t)$ and the velocity profiles in the sections that the wave has not reached yet differ somewhat from each other.

Comparing these results with the case for $\lambda = 0$ and $V_0 = 0$ [7], when $w(0,t) = 2w_A$, we note that in this case, the velocity does not even reach $8\ m/s\ (< 2w_A)$.

In the third conditional half-cycle, when the wave reaches the end of the section with a damper and returns to the beginning of the section, the increase in velocity $w(l,t)$ occurs only at the 24th time step, and then it decreases. This is due to the air chamber.

Over time, discontinuities of the second kind (derivatives of the function) at the front of the shock wave occur, and the velocity field gradually passes to a uniform distribution. At $t = 500\ l/c$, the maximum deviation of the velocity from w_A is 0.001.

According to the presented quasi-one-dimensional N.E. Zhukovsky model, the pressure gradient is proportional to the flow rate and considers friction forces. In this regard, in the first half-cycle, the pressure begins to drop at the end of the section, and these perturbations propagate against the direction of the x-axis (Fig. 4). In contrast to the case for $\lambda = 0$ and $V_0 = 0$, in this case, smoother pressure curves are formed. However, discontinuities of the second kind are evident at the wavefront.

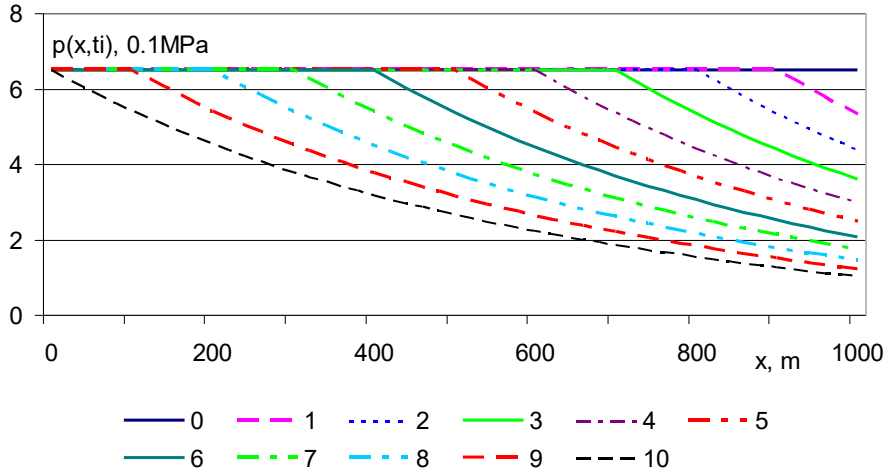

Fig. 4. Pressure distribution in first half-cycle with $l/(10c)$ time step.

The analysis showed that the discontinuities of the derivatives at the wavefront obey the Hugoniot relation for the total head [21]: a positive jump in the pressure derivative corresponds to a negative jump in the derivative w. In our case, this relation has the form $p + \frac{\rho w_*}{2} = const$. It is also fulfilled when the wave is reflected from the ends of the section.

Over time, jumps in pressure derivatives, as well as jumps in velocity derivatives, gradually decrease, and the process becomes a steady state one (Fig. 5).

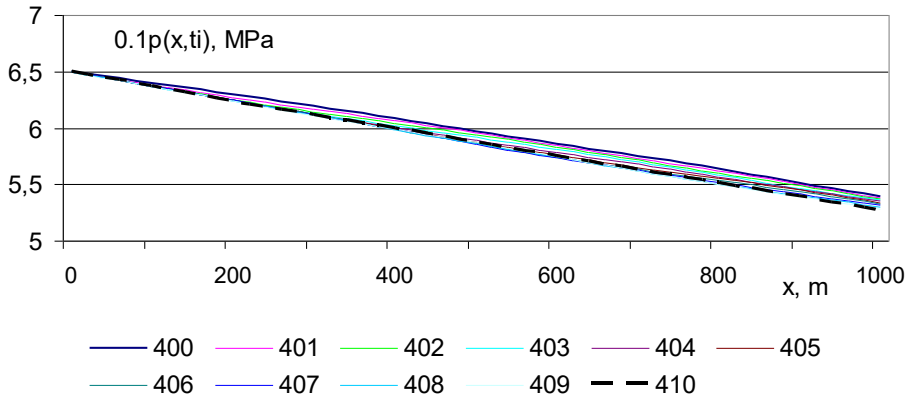

Fig. 5. Interval of pressure change along section length in 40th half-cycle.

Figures 6 and 7 show the changes in velocity and pressure in the sections for $V_0 = 0.001\ m^3$. It is seen from the figures that as $t \to \infty$, the velocity tends to its limit value W_A, and the pressure tends to its value in sections x according to the solution of the stationary problem for $w_0 = 5\ m/s$ and $p_{00} = 6.5\ MPa$. In this case, a linear pressure drop along the length of the section is clearly expressed: as $t \to \infty$ at an increase in distance, the pressure decreases linearly.

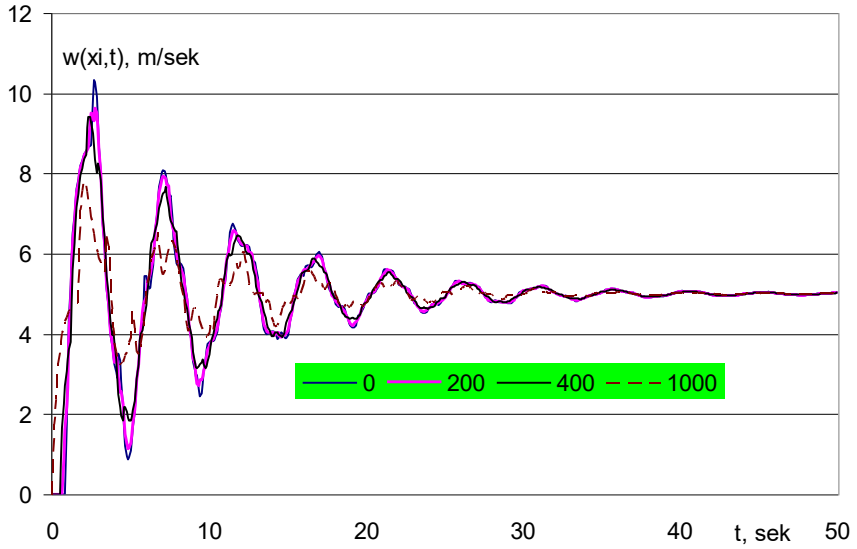

Fig. 6. Change in velocity over time in different sections. $V_0 = 0.001\ m^3$

From these graphs follows the presence of double extremes in half-periods, the nature of which should be substantiated in the future.

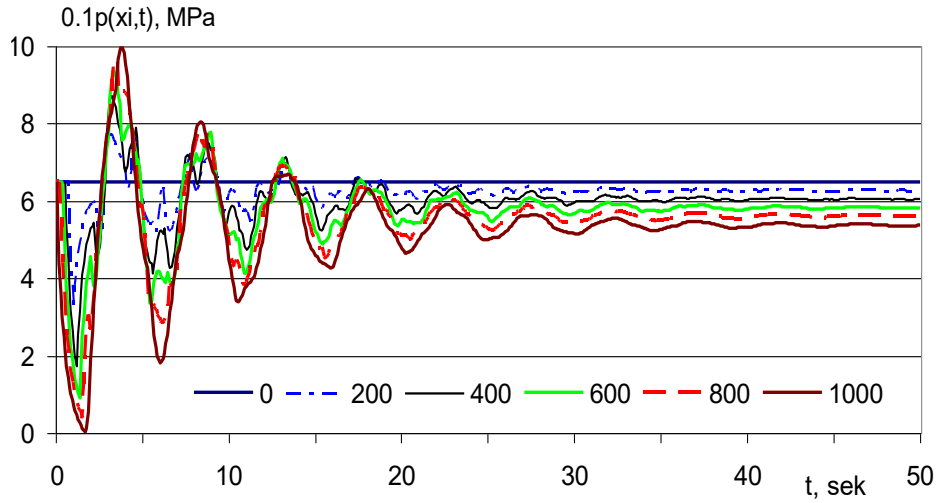

Fig. 7. Change in pressure over time in different sections for $V_0 = 0.001\ m^3$, $p_{00} = 6.5\ MPa$.

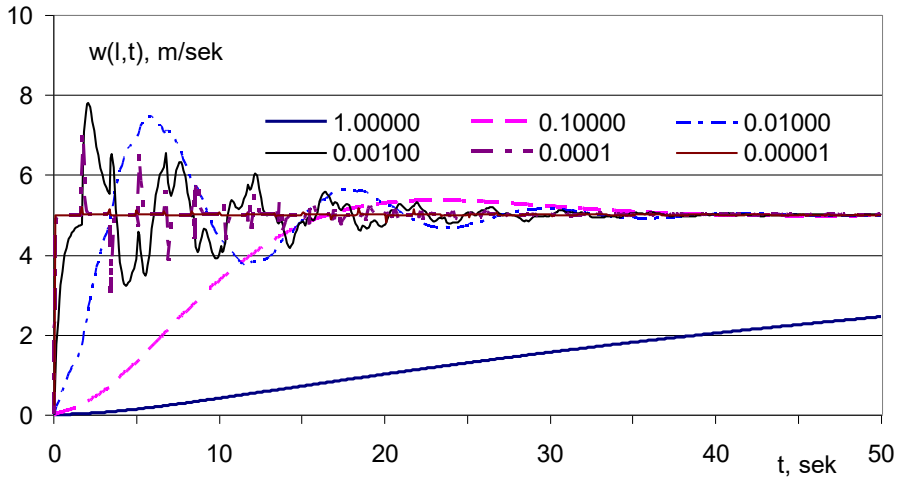

Fig. 8. Temporary change in exit velocity at different volumes of air chamber V_0 (m^3)

Figure 8 shows the changes in the velocity value at the end of the section for various values of the volume of the air chamber. The lower graphs reflect the end velocities at $V_0 = 1.000\ m^3$. These graphs are not finished since later they pass to the value of w_A. At large volumes of air chambers, steadying is slow. It can be seen that at the end of the section where the air chamber is installed, the amplitude of the disturbances is lower than in the inlet section despite the high difference at this end.

Graphs at $V_0 = 0.1\ m^3$ first increase from 0 to $5\ m/s$, and then the oscillatory process is damped. Two conditional maximums are clearly visible in the graphs.

More than three conditional maxima were observed in the graphs at $V_0 = 0.00100\ m^3$. As the damper volume decreases, the amplitude of velocity and pressure perturbations at the ends of the section increases, and the frequencies of the perturbations increase.

4 Conclusions

With an account for the air chamber installed at the end of the section, a mathematical model of the state of elementary inclined and horizontal sections of the pipeline is compiled when a constant pressure value is set at the inlet to the section.

The solution to the problem concerning velocity was obtained by the Fourier method, and the solution concerning pressure was determined by integrating the continuity equation.

The results of calculations obtained for a horizontal section for various values of the air chamber volume were discussed. It was determined that at a large volume of the air chamber, the transition from one mode of operation to another mode proceeds smoothly. With a decrease in the volume of the air chamber, velocity and pressure perturbations are formed due to the initiation and propagation of a compression shock wave. The frequency and amplitude of the disturbances increase as the volume in the air chamber decreases.

Based on the presented material, it can be concluded that for a given value of inlet pressure, it is possible to determine the volume of the air chamber, which ensures a smooth transition from one mode of operation in terms of flow rate to another mode.

References

1. V.E. Seleznev, V.V. Aleshin, S.N. Spinning. Mathematical modeling of pipeline networks and channel systems: methods, models, algorithms / Ed. V.E. Seleznev. - M .: MAKS Press, 2007, 695 p.
2. Deng Y. et al. A method for simulating the release of natural gas from the rupture of high-pressure pipelines in any terrain // Journal of Hazardous Materials Volume 342, 15 January 2018, Pages 418-428. https://doi.org/10.1016/j.jhazmat.2017.08.053
3. Michael V. Lurie. Modeling of Oil Product and Gas Pipeline Transportation WILEY-VCH Verlag GmbH & Co. KGaA, Weinheim, 2008. – 214 p.
4. Peining Yu., Yi Li., Jing Wei., YingXu., Tao Zhang. Modeling the pressure drop of wet gas in horizontal pipe // Chinese Journal of Chemical Engineering Volume 25, Issue 7, July 2017, Pages 829-837 https://doi.org/10.1016/j.cjche.2016.10.024
5. A. Lewandowski. New Numerical Methods for Transient Modeling of Gas Pipeline Networks. – NM: Pipeline Simulation Interest Group, 1995.
6. G.B. Whitham F.R.S. Linear and Nonlinear Waves. – NY: John Wiley & Sons, 1974
7. I.K. Khuzhaev, Kh.A. Mamadaliev, M.A. Kukanov. Analytical solution of the problem of the propagation of a compaction wave in an inclined pipeline caused by the deceleration of a fluid // Problems of computational and applied mathematics, Tashkent, 2015, №2, p.65-79.
8. V.V. Grachev, M.A. Huseynzade, B.I. Ksendz, E.I. Yakovlev. Complex piping systems. - M .: Nedra, 1982, 256 p.
9. V.V. Grachev, S.G. Shcherbakov, E.I. Yakovlev. Dynamics of pipeline systems. - M .: Nauka, 1987, 438 p.
10. Banda M.K., Herty M., Klar A. Gas flow in pipeline networks // Netw. Heterog. Media. Volume 1, Issue 1, Pages 41-56. https://bit.ly/2vKgGBQ
11. Khujaev I., Bozorov J., Akhmadjonov S. Investigation of the propagation of waves of sudden change in mass flow rate of fluid and gas in a “short” pipeline approach // 2019 IEEE Dynamics o Systems, Mechanisms and Machines (Dynamics). 05-07 Nov 2019 (Omsk, Russia)

12. I.A. Charny. Unsteady motion of real liquid in pipes. Ed. 2nd. - M .: Nedra, 1975, 296 p.
13. B.M. Budak, A.A. Samarski, A.N. Tikhonov. Sbornik zadach po matematicheskoi fizike. – M.: Nauka, 1972, 678 p.
14. A.N. Tikhonov, A.A. Samarski. Uravnenia matematicheskoi fiziki. – M: Nauka, 1972, 736 p.
15. Bermúdez A., López X., Vázquez-Cendón M.E. Treating network junctions in finite volume solution of transient gas flow models // Journal of Computational Physics. - 2017, Vol. 344, p187-209. doi https://doi.org/10.1016/j.jcp.2017.04.066
16. Ebrahimi-Moghadam A. et al. CFD analysis of natural gas emission from damaged pipelines: Correlation development for leakage estimation // Journal of Cleaner Production Volume 199, 20 October 2018, Pages 257-271. https://doi.org/10.1016/j.jclepro.2018.07.127.
17. Kurbatova G.I., Ermolaeva N.N. The Mathematical Models of Gas Transmission at Hyper-Pressure // Applied Mathematical Sciences, 2014. Vol. 8, No. 124. – P. 6191-6203. http://dx.doi.org/10.12988/ams.2014.47508
18. Zhenhua Rui, Guoqing Han, He Zhang, Sai Wang, Hui Puc, Kegang Ling A new model to evaluate two leak points in a gas pipeline // Journal of Natural Gas Science and Engineering Volume 46, October 2017, Pages 491-497
19. I. K. Khuzhaev, S. S. Akhmadjonov, and M. K. Mahkamov Modeling the Stages of Verification of the Suitability of a Short Section of a Gas Pipeline for Operation // Mathematical Models and Computer Simulations, 2022, Vol. 14, No. 6, pp. 972–983.
20. Kalitkin N.N. Numerical methods. – M.: Nauka, 1978. – 512 p.
21. Samarskii A.A., Popov Yu.P. Difference schemes of gas dynamics. – M.: Nauka, 1975. – 352 p.